Jurnal
Teknologi

Full Paper

QUANTITATIVE ANALYSIS OF ELECTRICAL CURRENT EFFECT ON MAGNETIC RESONANCE IMAGE TISSUE INTENSITY

Khusnul Ain[a], Lina Choridah[b], Deddy Kurniadi[c], Agah D. Garnadi[d], Utriweni Mukhaiyar[e], Nurhuda Hendra Setyawan[b]

[a]Biomedical Engineering Airlangga University, Indonesia
[b]Department of Radiology Faculty of Medicine, Public Health, and Nursing Universitas Gadjah Mada, Indonesia
[c]Department of Engineering Physics, Bandung Institute of Technology, Indonesia
[d]Mathematics and Sciences, Bogor Agriculture Institute, Indonesia
[e]Statistics Research Division, Faculty of Mathematics and Natural Sciences, Bandung Institute of Technology, Indonesia

Article history
Received
18 July 2022
Received in revised form
1 December 2022
Accepted
4 December 2022
Published Online
23 February 2023

*Corresponding author
linachoridah@ugm.ac.id

Graphical abstract

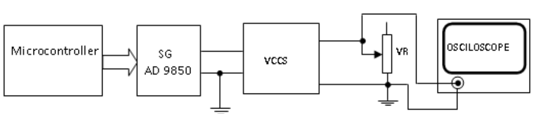

Abstract

Recent studies in magnetic resonance imaging (MRI) aim to improve image quality while reducing scan time. Electrical current injection in the form of magnetic resonance electrical impedance tomography (MREIT) is believed to be affecting image quality and scan time thus can improve the possibility of becoming a non-chemical contrast agent in MRI. This study will observe and analyze the effect of electrical current injection on a phantom object to determine whether there is a different tissue image intensity. A thigh of lamb was used as a biological tissue phantom. The scan was performed on both T1and T2-weighted without and with an electrical current injection of 0.5 mA Electrical current injection decreased mean of tissue image intensity on T1-weighted images on both muscle (1759 vs 794) and bone (2752 vs 1550) ($p<0.05$). On the other hand, the electrical current increased mean of tissue image intensity on T2-weighted images on both muscle (303 vs 897) and bone (579 vs 1499) ($p<0.05$). There is also a difference in tissue image intensity on both T1 and T2-weighted images with and without electrical current injection on bone and muscle. The implication of this difference in image quality is a subject for further study.

Keywords: Magnetic resonance imaging, Tissue image intensity, T1-weighted image, T2-weighted images, MREIT

1.0 INTRODUCTION

Since magnetic resonance imaging (MRI) was invented in the early 1970s, it has been widely used in medicine for diagnosis modality and massively developed by many researchers [1, 2, 3]. In MRI, the use of contrast agents is very useful to improve image quality on the object of observation. In the clinical field, until now there are two main ingredients commonly used as a contrast agent in MRI, namely Gadolinium (Gd) and iron oxides. Gadolinium is a paramagnetic element, whereas iron oxides are known as super paramagnetic materials [4, 5, 6]. The paramagnetic effect of Gd in contrast enhancement of MRI images is by decreasing the relaxation times of T2 and T1 on protons. With the use of iron oxide, the dephasing rate of T2 * increases as well as T2 and T1 in the protons [7, 8, 9].

MRI is very useful in evaluation of pregnant women, especially to detect common diseases, such as acute abdominal and pelvic pain or placental abnormalities, as well as neurological or fetal abnormalities, infections, or neoplasms. However, the concerns about negative impacts during the usage of MRI in pregnancy are rising, especially about the knowledge of administration of gadolinium-based contrast agents, is still limited. Gadolinium is a permeable substance which can cross the placenta, thus the administration of Gadolinium to pregnant women can be affected the fetus. On the other hand, no report of any harm from the excretion of a certain amount of Gadolium in form of breast milk, thus the administration of this agent can not interrupt breast feeding phase [10, 11, 12].

Apart from this, Gd also cannot be given to patients with impaired kidney function. Gadolinium-containing contrast agents may increase the risk of a rare but serious disease called nephrogenic systemic fibrosis in people with severe kidney failure [13, 14].

In recent years, many questions have arisen about the safety of this material as a contrast agent. This begins with the publication of Kanda *et al*. which states that there are spots of Gadolinium agent left in the patient's brain tissue after undergoing MRI scanning with contrast agent Gd. In addition, recent research also shows that there is a potential effect of Gd compounds which can cause necrosis and apoptosis in liver cells [15, 16, 17].

To overcome this, several studies were conducted to improve the quality of MRI images without using chemical contrast agents. Recent studies on MRI development aims to reduce in acquisition time and improve image resolution. For example, some studies about reduction acquisition time are echo-planar imaging (EPI) method, rapid acquisition with relaxation enhancement (RARE) method, accelerated fully sampled acquisition, and compressed sensing method. While some studies about improvement image resolution are super-resolution reconstruction (SRR) method and magnetic resonance electrical impedance tomography (MREIT) method [18].

MREIT is the injection of electrical current into an imaging object through electrodes when the MRI is scanning. In a biological object, this injection will affect the distribution of conductivity within the object. The electrical current will induce magnetic flux density. The MRI will process the magnetic flux density to form an image [19]. Basic of MREIT is the alteration of electrical conductivity distribution inside the biological object when injected with electrical current. This alteration is affected by molecular composition, cellular structure, concentration, and mobility of chemical components intracellular, extracellular fluids, and temperature [20, 21, 22].

Previous studies have found that MREIT could be an alternative as non-chemical contrast agent although having a poor signal-to-noise ratio (SNR) [23]. In our opinion, SNR should be evaluated along with other image quality parameters that can be measured, e.g., tissue image intensity. The aim of this study is to compare tissue image intensity without and with electrical current on MRI.

2.0 METHODOLOGY

2.1 VCCS (Voltage Converter Current Source)

A multi-frequency VCCS system with varying electrical current has been developed as a contrast agent in MRI. VCCS is the most commonly used current source in Bioimpedance Analysis systems due to its ability to provide a controllable electric current when injected into the load impedance. The multi-frequency VCCS system consists of a microcontroller, the AD 9850 programmable signal generator and the VCCS circuit shown in Figure 1.

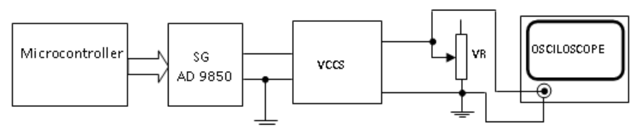

Figure 1 The VCCS multifrequency Sistem

The VCCS system is a Howland current source enhanced using dual Op-Amps. In order to obtain a stable output across the load, this VCCS uses matching resistors to complete the feedback. The current generated in this design is consistent in 0.05 mA to 1 mA. This VCCS design uses a dual Op-Amp OPA2134 in Figure 2.

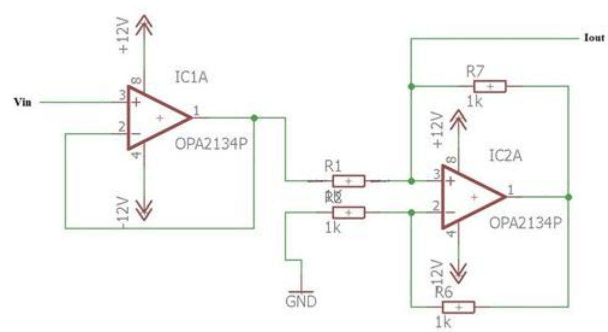

Figure 2 The VCCS schematic design

This VCCS uses 4 resistors of 1 kΩ. The first OP-Amp receives the signal from the High Pass Filter and forwards it to the second OP-Amp. Before being forwarded to the second Op-Amp, the first resistor is connected to the output of the first Op-Amp. The second resistor is connected to the negative pin of the second OP-Amp with ground. The third resistor is connected to the negative pin of the second op-amp and the output of the second op-amp. The fourth resistor is connected to the positive pin of the second

Op-Amp and the output of the second Op-Amp. The output current is injected into the variable resistor (VR) as a load.

2.2 Phantom Imaging

This study used a thigh of lamb as the phantom for MRI scanning. The tight of lamb phantom consisted of muscle and bone to represent the human body. The image acquisition used 1.5 Tesla Philips Multiva MR scanner with parameters as follows: repetition time (T= 668 ms), echo time (TE = 15 ms), number of echoes (NER = 1), field of view (FOV 100 × 100 mm), number of excitations (NEX 1), and imaging matrix 640 × 640. The phantom was scanned without electrical current and with 0.5mA electrical current injected by two flexible electrodes around the phantom. The scan sequences used in this research were T1-weighted images and T2-weighted images. The image acquisition process is shown in Figure 3.

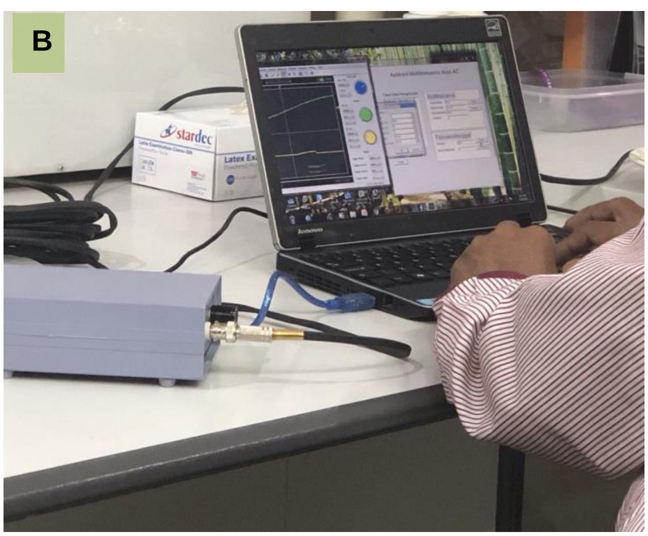

Figure 3 (A). Thigh of lamb was used as biological phantom object. Due to its small size, pediatric head coil was used with body coil to provide better signal-to-noise ratio. (B). A multi-frequency electrical current generator was connected to the phantom using electrodes and was controlled from operator room, just outside the scanner room

2.3 Data Analysis

We processed the images using RadiAnt DICOM Viewer to obtain the mean number of signal intensities. We divided the images into three parts, background, muscle, and bone. We used 25 regions of interest (RoI) for each part and recorded all the mean number of signal intensities. The RoI size was 0.3 cm² for the muscle and 0.06 cm² for the bone [24]. The raw RoI placements were shown in Figure 4. After the data collected, we tested the data normality using Saphiro-Wilk normality test and compared the means using T-test and Wilcoxon test.

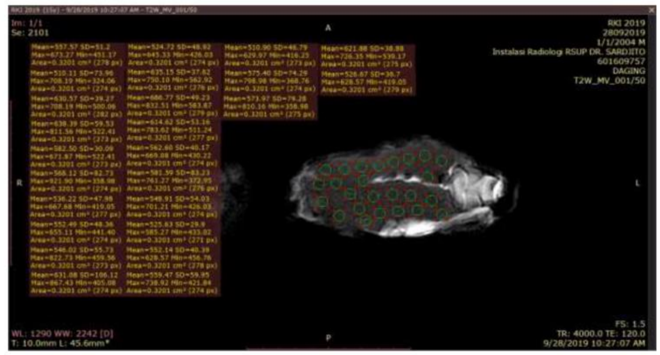

Figure 4 Twenty-five region of interests (RoI) were placed in muscle area and the mean number were recorded to get the average muscle tissue signal intensity of this T2-weighted image. This procedure were repeated for bone and background noise area.

3.0 RESULTS AND DISCUSSION

Figure 2 shows I_{out} is the output current signal from the VCCS and V_{in} is the input to VCCS from the voltage generator. The voltage signal from the current injection observed is Vrms. This circuit uses 1 kΩ resistor before being applied to the load, so that the formula for finding the current is $I = \frac{V_{IN}}{1000}$

The output signal from the generator is easily distorted if it is connected directly to the VCCS. Due to the high output impedance of the generator circuit, it used a voltage buffer to transfer the generator voltage to a VCCS which has a relatively low input impedance. The curve of the stability of the VCCS trial is shown in Figure 5.

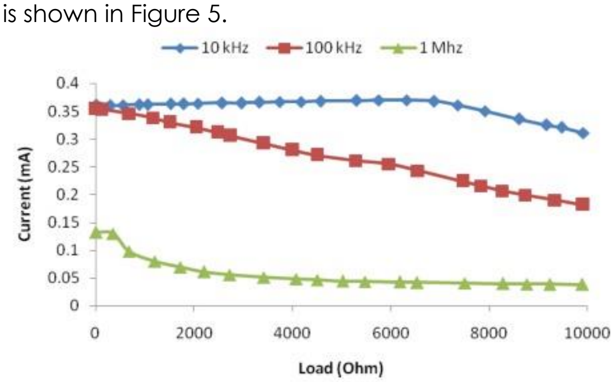

Figure 5 The curve of load versus output current from VCCS in 10 kHz, 100 kHz and 1 MHz

At a frequency of 10 kHz, VCCS produces a stable current of 0.36 mA with a maximum load of 6 kΩ and the current decreases to 0.31 mA at a load of 10 kΩ. At a frequency of 100 kHz from a load of 0 to 10 kΩ the current drops from 0.35 mA to 0.18 mA. At a frequency of 1 MHz from a load of 0 to 341 Ω the current decreases to 0.051 mA. At a frequency of 10 kHz and 100 kHz, currents are obtained that can be used and are safe for the body because they are still in the range of 0.05 mA to 0.5 mA. However, at a frequency of 1 MHz when the load is more than 341 Ω the current is below the minimum limit of less than 0.05 mA so this frequency cannot be used because it will read inaccurately.

Raw images from T1-weighted and T2-weighted images both with and without electrical current injection were shown in Figure 6.

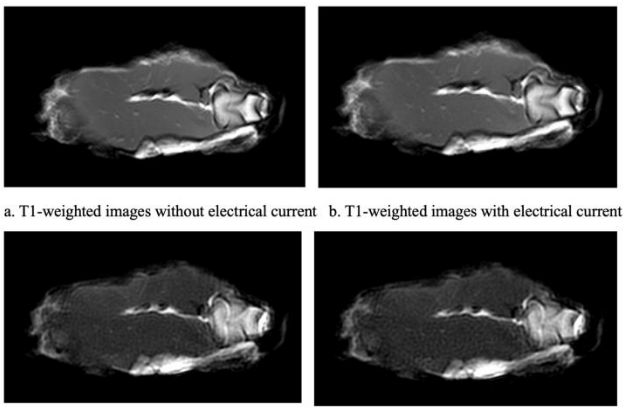

a. T1-weighted images without electrical current b. T1-weighted images with electrical current

c. T2-weighted images without electrical current. d. T2-weighted images with electrical current

Figure 6 Images here shown different tissue image intensity with and without electrical current injection. Both T1-weighted and T2-weighted images experienced tissue signal intensities changes due to electrical current introduction, with T1-weighted images appeared darker (lower signal intensity) and T2-weighted images appeared brighter (higher signal intensity)

1. Image intensity data of phantom before applying electrical current

Based on the scatter diagram and the correlation value in Figure 7 and Table 1, the relationship between variables observed in the T1-weighted images before being given the current, has a correlation value that is not too large, as seen from the significance of the p-value which is greater than 10%. It can be said that there is no linearity pattern of the relationship between variables. Although not very large, the relationship in the opposite direction is indicated by the value of the standard deviation of the intensity between the background and the bone, which is indicated by the negative correlation value (r = -0.210).

As in the T1-weighted images, the relationship between the variables involved in the T2-weighted images also did not show a significant linearity pattern (Figure 8 and Table 2). The indication of a linear relationship in the opposite direction is shown by the mean muscle intensity with the background (r = -0.247) and the standard deviation of the background intensity with bone (r = -0.183). However, this value is small enough that it tends to be neglected.

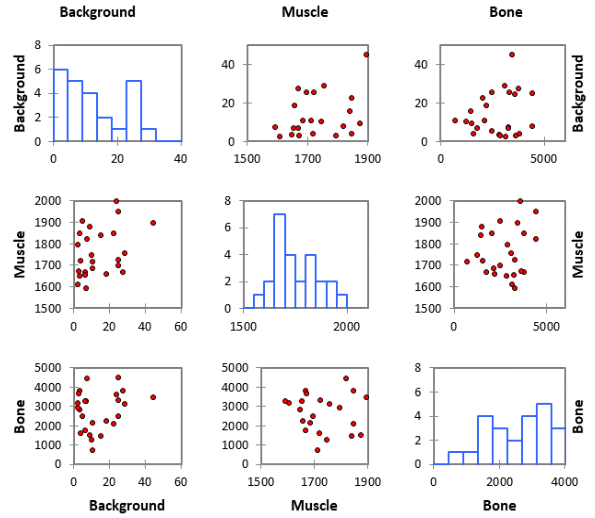

(a)

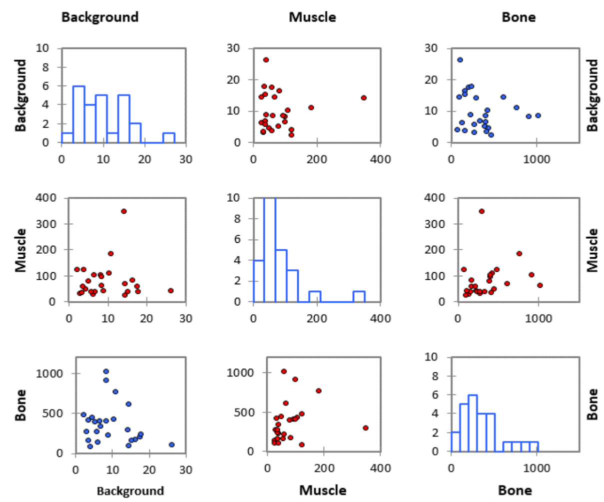

(b)

Figure 7 Scatter diagram of the mean (a) and standard deviation (b) of the intensity of the image on the background, muscles, and bones before applying currents to T1-weighted images

Table 1 The value of correlation and significance (p-value) of the relationship between variables before applying currents to T1-weighted images. Significance of the correlation for the mean intensity (lower triangle) and standard deviation of intensity (upper triangle).

Correlation (p-value)	Background	Muscle	Bone
Background	**1**	0.041 (0.847)	-0.210 (0.313)
Muscle	0.355 (0.082)	**1**	0.206 (0.324)
Bone	0.216 (0.301)	0.163	**1**

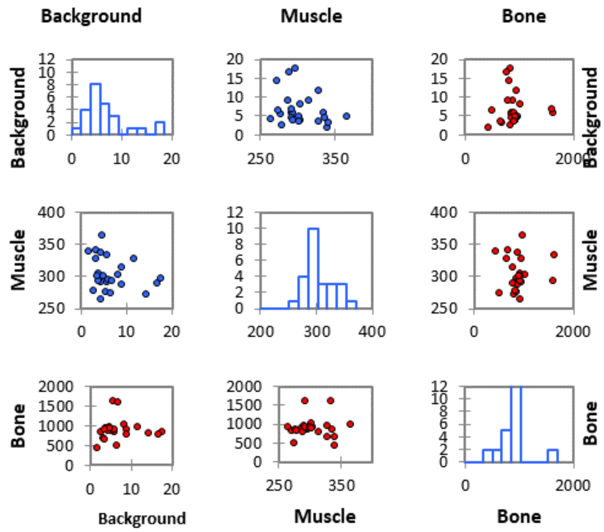

(a)

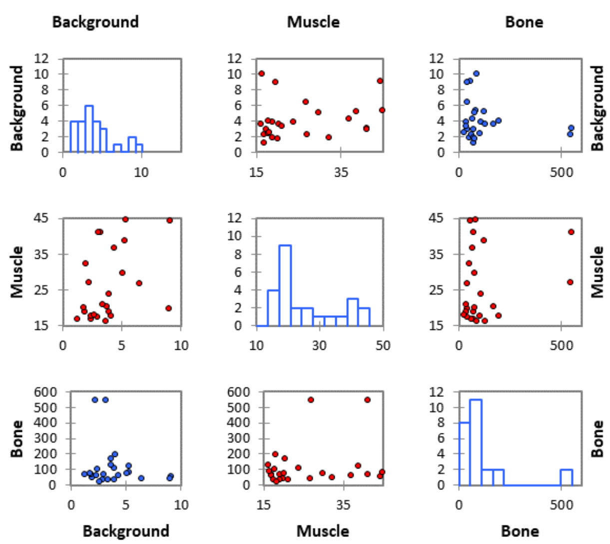

(b)

Figure 8 Scatter diagram of the mean (a) and standard deviation (b) of the intensity of the image on the background, muscles, and bones before applying currents to T2-weighted images

Table 2 The value of correlation and significance (p-value) of the relationship between variables before applying currents to T2-weighted images. Significance of the correlation for the mean intensity (lower triangle) and standard deviation of intensity (upper triangle)

Correlation (p-value)	Background	Muscle	Bone
Background	1	0.220 (0.290)	-0.183 (0.382)
Muscle	-0.247 (0.235)	1	0.220 (0.292)
Bone	0.040 (0.848)	0.031 (0.884)	1

2. *Image intensity data of phantom after applying electrical current*

Based on the correlation value and p-value obtained, the mean and background muscle intensity values have a significant correlation (r = 0.346) for the significance level α ≥ 10%. As for the standard deviation value, there is no linear relationship which is quite significant. An opposite linear relationship was indicated from the standard deviation of background and bone (r = -0.256), although it was not significant (shown in Figure 9 and Table 3).

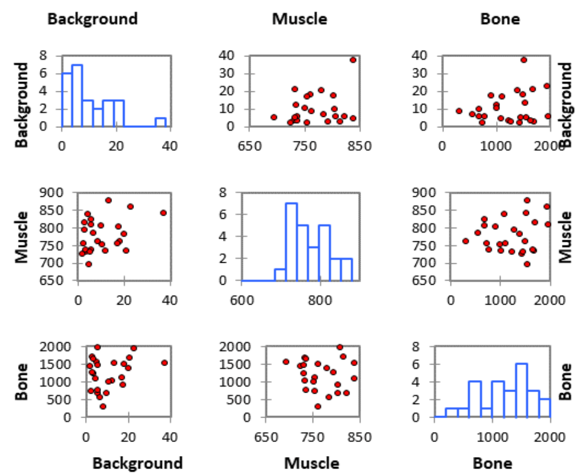

(a)

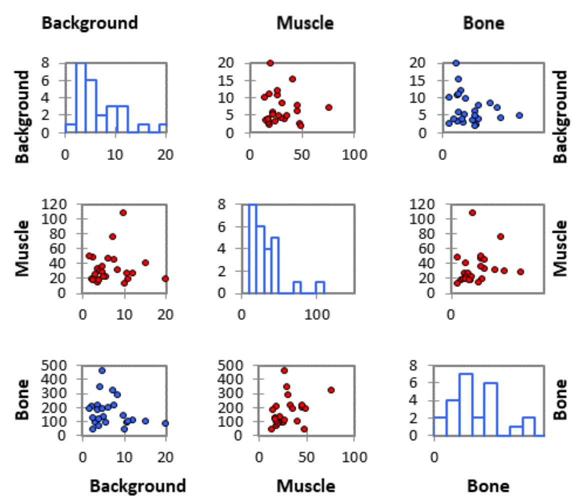

(b)

Figure 9 Scatter diagram of the mean (a) and standard deviation (b) of the intensity of the image on the background, muscles, and bones after applying currents to T1-weighted images

Table 3 The value of correlation and significance (p-value) of the relationship between variables after applying currents to T1-weighted images. Significance of the correlation for the mean intensity (lower triangle) and standard deviation of intensity (upper triangle)

Correlation (p-value)	Background	Muscle	Bone
Background	**1**	0.065 (0.756)	-0.256 (0.216)
Muscle	**0.346 (0.090)**	**1**	0.213 (0.307)
Bone	0.235 (0.259)	0.117 (0.579)	**1**

In T2-weighted images after given electrical current, there is a significant linear relationship on the standard deviation of muscle and bone intensity, (r = 0.464) for $\alpha \geq 2\%$. The opposite direction linear relationship is seen between the mean background intensity with muscle (r = -0.304) for significance $\alpha > 14\%$. This opposite relationship shows that the greater the mean muscle eating intensity, the smaller the mean background intensity (shown in Figure 10 and Table 4).

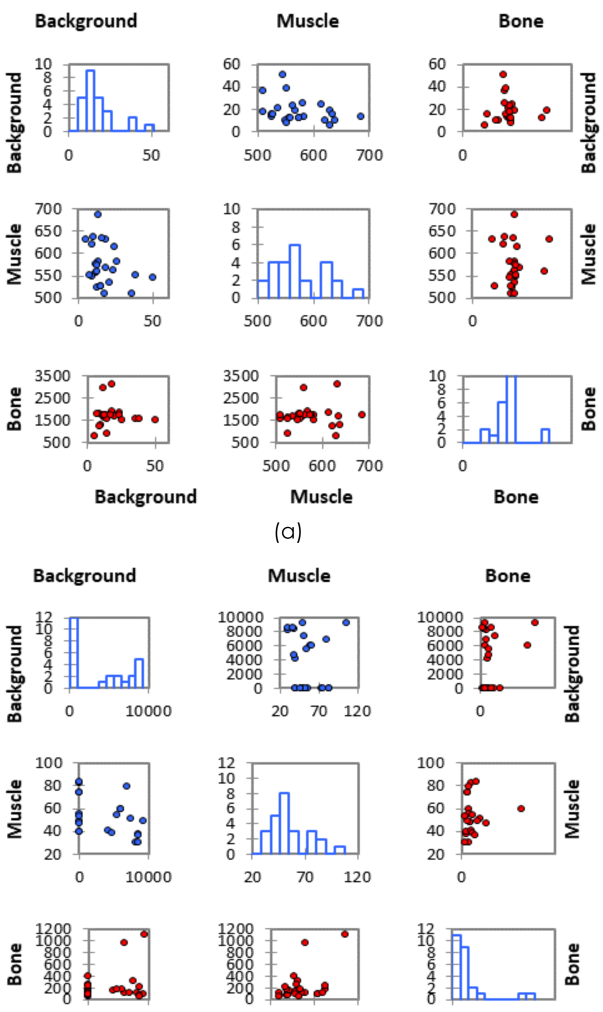

(a)

(b)

Figure 10 Scatter diagram of the mean (a) and standard deviation (b) of the intensity of the image on the background, muscles, and bones after applying currents to T2-weighted image

Table 4 The value of correlation and significance (p-value) of the relationship between variables after applying currents to T2-weighted images. Significance of the correlation for the mean intensity (lower triangle) and standard deviation of intensity (upper triangle)

Correlation (p-value)	Background	Muscle	Bone
Background	**1**	-0.126 (0.549)	0.268 (0.195)
Muscle	-0.304 (0.140)	**1**	**0.464 (0.019)**
Bone	0.007 (0.974)	0.058 (0.785)	**1**

The existence of several relationships between variables that become significant when given current, indicates the effect of giving electrical current on the mean tissue signal intensity [25,26]. Therefore, a hypothesis test (T-test) was carried out to check for a significant difference in the mean intensity before and after being given the current, with the null hypothesis that no change occurred, that is, the current application had no impact. The results of the hypothesis test are summarized in Table 5.

Based on the hypothesis test conclusion of Table 5, it can be seen that, except for the mean background intensity on T1-weighted images, all variables experienced a significant change in the mean intensity before and after the current was applied. This shows that the application of current gives a change in the mean intensity on the background with T2-weighted images, as well as in muscles and bones in both T1- and T2--weighted images [27].

Table 5 Hypothesis testing for both T1- and T2-weighted images tissue signal intensity changes before and after electrical current was applied to the biological phantom object

	T1			T2		
	Background	**Muscle**	**Bone**	**Background**	**Muscle**	**Bone**
$\bar{X}_1$	13.94	1759.32	2752.43	6.68	303.90	897.16
S_1^2	122.77	12333.13	1020521.96	17.59	652.44	65437.72
$\bar{X}_2$	10.53	777.44	1,227.05	17.81	574.14	1,700.80
S_2^2	72.88	2228.01	195852.86	109.37	2109.68	226113.96
n	25	25	25	25	25	25
degree of freedom	45	32	33	32	38	37
α	0.05	0.05	0.05	0.05	0.05	0.05
t-table	2.01	2.04	2.04	2.04	2.03	2.03
t-statistics	1.22	40.69	6.92	-4.94	-25.71	-7.44
p-value	0.23	0.00	0.00	0.00	0.00	0.00
Conclusion	H0 is not rejected	H0 is rejected	H0 is rejected	H0 is rejected	H0 is rejected	H0 is rejected

This study shows each image group is entirely different; in T1-weighted images, the mean of tissue image intensity is significantly decreased in the electrical current group. This result is similar to the previous research that concludes although MREIT has poor SNR and low spatial resolution but has potential to be a non-chemical contrast agent [28,29,30]. Meanwhile, in T2-weighted images, the mean of tissue image intensity is significantly increased in the electrical current group. This result supports the theory of MREIT that can increase the signal intensity of MR images and its quality [31]. This inconsistent result is a subject for further study.

Unlike the previous research, this MREIT study was done without image reconstruction using the algorithm, e.g., *J*-substitution algorithm or single-step harmonic *Bz* algorithm [32]. This study also did not use SNR as the standard image quality parameter because the previous studies found that the SNR of MREIT were poor.

4.0 CONCLUSION

There is a significant tissue image intensity difference with and without electrical current application in both T1- and T2-weighted MR images of muscle and bone.

Although this study found that the result of tissue intensity images is significantly different, it does not conclude which one is better. Therefore, there is a need to evaluate and validate comparison between the MR images without and with electrical current by experienced clinical radiologists.

The evidence that electrical current injection can alter image properties in MR examination is a promising finding for future researches. More studies need to be done in order to optimize the EIT parameters, verify the images, and assess its applicability in clinical settings.

Acknowledgement

The authors would like to express gratefulness to the Indonesian Ministry of Research and High Education by Institution of Research and Innovation for funding this research through the RKI Project 2019 and 2020.

References

[1] Rinck, P. 2018. *Magnetic Resonance in Medicine*. 12th ed. Norderstedt, Germany: Books on Demand.

[2] Daniel Harris Lynn McNicoll, M. D., Gary Epstein-Lubow, M. D., and Kali, S. Thomas, B. A. 2019. Value of MRI in Medicine: More than Just Another Test? *Physiology & Behavior*. 176(1): 139-148. https://doi.org/10.1002/jmri.26211.

[3] Khan, S. U., Ullah, N., Ahmed, I., Ahmad, I., & Mahsud, M. I. 2018. MRI Imaging, Comparison of MRI with other Modalities, Noise in MRI Images and Machine Learning Techniques for Noise Removal: A Review. *Current Medical Imaging Formerly Current Medical Imaging Reviews*. 15(3): 243–254. Doi: https://doi.org/10.2174/1573405614666180726124952.

[4] Xiao, Y. D., R. Paudel., J. Liu., C. Ma., Z. Zhang., and K. Zhou. 2016. MRI Contrasts Agents: Classification and Application (Review). *International Journal of Molecular Medicine*. 38: 1319-1326. Doi: https://doi.org/10.3892/ijmm.2016.2744.

[5] Ibrahim, M. A., Hazhirkarzar, B., Dublin, A. B. 2022. Gadolinium Magnetic Resonance Imaging. *StatPearls.* [Internet]. Treasure Island (FL): StatPearls Publishing. Available from: https://www.ncbi.nlm.nih.gov/books/NBK482487/.

[6] Delgado, A. F., Westen, D. Van, Nilsson, M., Knutsson, L., & Sundgren, P. C. 2019. Diagnostic Value of Alternative Techniques to Gadolinium-Based Contrast Agents in MR Neuroimaging — A Comprehensive Overview. *Insights into Imaging.* 10(84): 1-15. Doi: https://doi.org/10.1186/s13244-019-0771-1.

[7] Andrade, K. N., G. Arizaga., and J. Mayorga. 2020. Effect of Gd and Dy Concentrations in Layered Double Hydroxides on Contrast in Magnetic Reconance Imaging. *Multidisciplinary Digital Publishing Institute*. 8(4): 462. Doi: https://doi.org/10.3390/pr8040462.

[8] Kawahara, D., & Nagata, Y. 2021. T1-Weighted and T2-Weighted MRI Image Synthesis with Convolutional Generative Adversarial Networks. *Reports of Practical Oncology and Radiotherapy*. 26(1): 1-2. Doi: https://doi.org/10.5603/RPOR.a2021.0005.

[9] ouhsina, N., Decante, C., Hardel, J. B., Rouleau, D., Abadie, J., Hamel, A., Visage, C. Le, Lesoeur, J., & Region-of-interest, R. O. I. 2022. Comparison of MRI T1, T2, and T2 Mapping with Histology for Assessment of Intervertebral Disc Degeneration in an Ovine Model. *Scientific Reports.* 1-12. Doi: https://doi.org/10.1038/s41598-022-09348-w.

[10] Rogosnitzky, M., and S. Branch. 2016. Gadolinium-Based Contrast Agent Toxicity: A Review of Known and Proposed

Mechanism. *National Library of Medicine*. 29(3): 365-76. Doi: 10.1007/s10534-016-9931-7.

[11] Gatta, G., Di Grezia, G., Cuccurullo, V., Sardu, C., Iovino, F., Comune, R., Ruggiero, A., Chirico, M., La Forgia, D., Fanizzi, A., Massafra, R., Belfiore, M. P., Falco, G., Reginelli, A., Brunese, L., Grassi, R., Cappabianca, S., & Viola, L. 2022. MRI in Pregnancy and Precision Medicine: A Review from Literature. *Journal of Personalized Medicine*. 12(1). Doi: https://doi.org/10.3390/jpm12010009.

[12] Jain, C. 2019. ACOG Committee Opinion Guidelines for Diagnostic Imaging during Pregnancy and Lactation. *Obstetrics and Gynecology*. 133(1): 186. Doi: https://doi.org/10.1097/AOG.0000000000003049.

[13] Guo, B.J., Z. Yang., and L. Zhang. 2018. Gadolinium Deposition in Brain: Current Scientific Evidence and Future Perspectives. *National Library of Medicine*. 11: 335.

[14] Ramalho, J., M. Ramalho., M. Jay., L. Burke., and R. Semelka. 2016. Gadolinium Toxicity and Treatment. *Magnetic Resonance Imaging*. 34(1): 1394-1398. Doi: https://doi.org/10.1016/j.mri.2016.09.005.

[15] Kanda, T., K. Ishii., H. Kawaguch, K. Kitajima, and D. Takenaka. 2014. High Signal Intensity in the Dentate Nucleus and Globus Pallidus on Unenhanced T1-weighted MR Images: Relationship with Increasing Cumulative Dose of a Gadolinium-based Contrast Material. *Radiology*. 270(3): 834-841. Doi: 10.1148/radiol.13131669.

[16] Mercantepe, T., Tumakaya, L., Celiker, F, B., Suzan, Z, T., Cinar, S., Akyildiz, K., Mercantepe, F., Yilmaz, A. 2018. Effects of Gadolinium-based MRI Contrast Agents on Liver Tissue. *J Magn Reson Imaging*. 48(5): 1367-1374. Doi: https://doi.org/10.1002/jmri.26031.

[17] Klein, A, D., Oyarzun, J, E., Cortez, C., Zanlungo, S. 2018. Gadolinium Chloride Rescues Niemann-Pick Type C Liver Damage. *Int J Mol Sci*. 19(11): 3599. Doi: 10.3390/ijms19113599.

[18] Joy, M., G. Scott., and M. Henkelman, 1989. M. In Vivo Detection of Applied Electric Currents by Magnetic Resonance Imaging. *Magnetic Resonance Imaging*. 7(1): 89-94. Doi: 10.1016/0730-725x(89)90328-7.

[19] Grimnes, S. and O. Martinsen. 2015. *Bioimpedance and Bioelectricity Basics*. London, U.K: Academic Press.

[20] Kim, H. J., Y. Kim., A. Minhas., W. Jeong., E. Woo., J. Seo., and O. Kwon. 2009. In Vivo High-Resolution Conductivity Imaging of the Human Leg Using MREIT: The First Human Experiment. *IEEE Transactions on Medical Imaging*. 28(11): 1681-1687. Doi: 10.1109/TMI.2009.2018112.

[21] Eroglu, H. H., Sadighi, M., & Eyuboglu, B. M. 2018. Induced Current Magnetic Resonance Electrical Conductivity Imaging with Oscillating Gradients. *IEEE transactions on Medical Imaging*. 37(7): 1606-1617. Doi: https://doi.org/10.1109/TMI.2018.2795718.

[22] Dominik Garmatter and Bastian Harrach. 2018. Magnetic Resonance Electrical Impedance Tomography (MREIT): Convergence and Reduced Basis Approach. *SIAM J. Img. Sci*. 11(1): 863-887. Doi: https://doi.org/10.1137/17M1155958.

[23] Oh, S., J. Han., S. Lee, M. Cho, B. Lee., and E. Woo. 2003. Electrical Conductivity Imaging by Magnetic Resonance Electrical Impedance Tomography (MREIT). *Magnetic Resonance in Medicine*. 50(4): 875-878. Doi: https://doi.org/10.1002/mrm.10588.

[24] Ain, K., D. Kurniadi, M. Ulum, L. Choridah, U. Mukhayyar, A. Garnadi, N. Setyawan, and B. Ariwanto. 2022. Development of Multi Frequency Electrical Impedance Tomography for Rectangular Geometry by Finite Volume Methods. *Jurnal Teknologi*. 84(2): 9-15. Doi: https://doi.org/10.11113/jurnalteknologi.v84.16936.

[25] Janssen, I., S. Heymsfield., and R. Baumgartner. 2000. Estimation of Skeletal Muscle Mass by Bioelectrical Impedance Analysis. *National Library of Medicine*. 89(2): 465-71. Doi: 10.1152/jappl.2000.89.2.465.

[26] Lukaski, H. C., P. Johnson, W. Bolonchuk, and G. Lykken. 1985. Assessment of Fat-free Mass using Bioelectrical Impedance Measurements of Human Body. *National Library of Medicine*. 41(4): 810-7. Doi: https://doi.org/10.1093/ajcn/41.4.810.

[27] Kapanen, M., and M. Tenhunen. 2012. T1/T2*-weighted MRI Provides Clinically Relevant Pseudo-CT Density Data for the Pelvic Bones in MRI-Only Based Radiotherapy Treatment Planning. *Acta Oncologica*. 52(3): 612-618. Doi: https://doi.org/10.3109/0284186X.2012.692883.

[28] Muftuler, L. T., M. Hamamura, O. Birgul, and O. Nalcioglu. 2004. Resolution and Contrast in Magnetic Resonance Electrical Impedance Tomography (MREIT) and Its Application to Cancer Imaging. *Technology in Cancer Research & Treatment*. 3(6): 599-609. Doi: https://doi.org/10.1177/153303460400300610.

[29] Song, Y., W. Jeong., E. Woo., and J. Seo. 2016. A Method for MREIT-based Source imaging: Simulation Studies. *Physics in Medicine & Biology*. 61: 5706-5723. Doi: http://dx.doi.org/10.1088/0031-9155/61/15/5706.

[30] Hellige, N.C., B. Meyer., T. Rodt., and J. Claussen. 2012. In-Vitro Evaluation of Contrast Media for Assessment of Regional Perfusion Distribution by Electrical Impedance Tomography (EIT). *Biomedical Engineering/ Biomedizinische Technik*. 57(Suppl.1). Doi: 10.1515/bmt-2012-4442.

[31] Arpinar, V. E., M. Hamamura., E. Degirmenci., and L. Muftuler. 2012. MREIT Experiments with 200µA Injected Currents: A Feasibility Study Using Two Reconstruction Algorithms, SMM and Harmonic BZ. *National Library of Medicine*. 57(13): 4245-4261. Doi: https://dx.doi.org/10.1088%2F00319155%2F57%2F13%2F4245.

[32] Jeon, K., C. Lee, and E. Woo. 2017. A Harmonic BZ-Based Conductivity Reconstruction Method in MREIT with Influence of Non-transversal Current Density. *Inverse Problems in Science and Engineering*. 26(6): 811-833. Doi: https://doi.org/10.1080/17415977.2017.1352587.